Wang XH, He YG, Li TZ. Neural network algorithm for designing FIR filters utilizing frequency-response masking technique. JOURNAL OF COMPUTER SCIENCE AND TECHNOLOGY 24(3): 463–471 May 2009

Neural Network Algorithm for Designing FIR Filters Utilizing Frequency-Response Masking Technique

Xiao-Hua Wang[1,2] (王小华), Yi-Gang He[2] (何怡刚), and Tian-Zan Li[1] (李天赞)

[1] *Department of Electrical and Information Engineering, Changsha University of Science and Technology Changsha 410004, China*

[2] *Department of Electrical and Information Engineering, Hunan University, Changsha 410082, China*

E-mail: cslgwxh@yahoo.com.cn; hyghnu@yahoo.com.cn

Received May 20, 2008; revised November 25, 2008.

Abstract This paper presents a new joint optimization method for the design of sharp linear-phase finite-impulse response (FIR) digital filters which are synthesized by using basic and multistage frequency-response-masking (FRM) techniques. The method is based on a batch back-propagation neural network algorithm with a variable learning rate mode. We propose the following two-step optimization technique in order to reduce the complexity. At the first step, an initial FRM filter is designed by alternately optimizing the subfilters. At the second step, this solution is then used as a start-up solution to further optimization. The further optimization problem is highly nonlinear with respect to the coefficients of all the subfilters. Therefore, it is decomposed into several linear neural network optimization problems. Some examples from the literature are given, and the results show that the proposed algorithm can design better FRM filters than several existing methods.

Keywords frequency-response masking, FIR digital filter, neural network, optimal design

1 Introduction

Digital signal processing techniques are being applied to wireless communication systems, digital TVs, and multimedia system, which have resulted in a demand for narrow transition-width linear-phase finite-impulse response (FIR) digital filters. One of the most efficient approaches to synthesize narrow transition band linear-phase FIR digital filters is the frequency-response masking (FRM) technique. This approach produces filters with very sparse coefficient vectors and hence reduces the number of multipliers and adders required for tremendous implementation compared with conventional direct design methods. As a result, in many cases, it has become preferable primarily because if considerably reduces realization complexity compared with the other options[1−3].

Several designs for FRM filters have been investigated in the past, among which, the subfilters are optimized separately[4−8]. This produces only suboptimal solutions, thereby very likely to lead to poor overall solutions. Recently, several joint optimization methods have been developed (see [9–16]). In [9–12], two genetic algorithms, a second-order cone programming approach and a two-step optimization technique are introduced, respectively. These methods were proposed for simultaneously optimizing subfilters. The main difficulty is that they need to minimize some objective functions, which have a high degree of nonlinearity with respect to the coefficients of the subfilters. In [13], Lu W S and Hinamomoto T presented a semidefinite programming (SDP) approach in which the set of FRM filter coefficients of all the subfilters is treated as a single design vector, and an optimal FRM filter can be designed by using a sequence of linear updates of the design variables. The SDP method is readily extended to multistage FRM filter design. However, a problem with the method is the large number of constraints that inevitably affect design efficiency and, in the case of high-order FRM filters, may cause numerical difficulties. In [14–16], a weighted least squares (WLS) method is used for designing linear-phase FRM filters. In [14], the original least squares (LS) problem is decomposed into two linear LS problems when designing basic structure of FRM filters. In [15], the original LS problem is decomposed into four linear LS problems. In [16], the WLS

Short Paper

This work is supported by the National Natural Science Foundation of China under Grant Nos. 50677014 and 60876022, the Doctoral Special Fund of Ministry of Education of China under Grant No. 20060532002, the National High-Tech Research and Development 863 Program of China under Grant No. 2006AA04A104, and the Foundation of Hunan Provincial Natural Science Foundation of China under Grant No. 07JJ5076.

method was used for designing multistage FRM filters. The main advantage is that the highly WLS nonlinear problem with respect to the coefficients of the subfilters is decomposed into several linear LS problems.

This paper introduces a joint optimization method for the design of linear-phase FIR digital filters using the FRM technique. The method is based on a batch back-propagation neural network algorithm (BBPNNA) in which the highly nonlinear problem with respect to the coefficients of the subfilters is decomposed into several linear neural network optimization problems.

2 FRM Filter Structure and Frequency Response

As can be seen in Fig.1, the linear-phase FIR filter transfer function of the basic FRM structure is constructed as follows:

$$H(z) = H_{\rm a}(z^M)H_{\rm ma}(z) + [z^{-0.5M(N_{\rm a}-1)} - H_{\rm a}(z^M)]H_{\rm mc}(z), \tag{1a}$$

where

$$H_{\rm a}(z) = \sum_{n=0}^{N_{\rm a}-1} h_{\rm a}(n)z^{-n}, \tag{1b}$$

$$H_{\rm ma}(z) = \sum_{n=0}^{N_{\rm ma}-1} h_{\rm ma}(n)z^{-n}, \tag{1c}$$

$$H_{\rm mc}(z) = \sum_{n=0}^{N_{\rm mc}-1} h_{\rm mc}(n)z^{-n}. \tag{1d}$$

The impulse response coefficients $h_{\rm a}(n)$, $h_{\rm ma}(n)$, and $h_{\rm mc}(n)$ are symmetrical. If all subfilters have linear-phase response with $N_{\rm ma}$ and $N_{\rm mc}$ either both even or both odd and $(N_{\rm a}-1)M$ even, then the FRM filter has a linear-phase response.

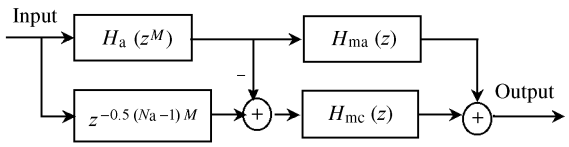

Fig.1. Basic FRM filter structure.

The zero-phase frequency response of $H(z)$ (the group delay $D = (N_{\rm a}-1)M/2 + \max\{(N_{\rm ma}-1)/2, (N_{\rm mc}-1)/2\}$ is omitted) can be expressed as

$$\begin{aligned} H(\boldsymbol{\omega}) &= [\boldsymbol{a}_{\rm a}^{\rm T}\boldsymbol{c}_{\rm a}(\omega)][\boldsymbol{a}_{\rm ma}^{\rm T}\boldsymbol{c}_{\rm ma}(\omega) - \boldsymbol{a}_{\rm mc}^{\rm T}\boldsymbol{c}_{\rm mc}(\omega)] \\ &\quad + \boldsymbol{a}_{\rm mc}^{\rm T}\boldsymbol{c}_{\rm mc}(\omega) \\ &= H_{\rm a}(\omega)[H_{\rm ma}(\omega) - H_{\rm mc}(\omega)] + H_{\rm mc}(\omega), \end{aligned} \tag{2a}$$

where

$$\boldsymbol{a}_{\rm a} = \begin{cases} [h_{\rm a}((N_{\rm a}-1)/2)\ 2h_{\rm a}((N_{\rm a}+1)/2)\ \cdots \\ \quad 2h_{\rm a}(N_{\rm a}-1)]^{\rm T}, & \text{if } N_{\rm a} \text{ is odd;} \\ 2[h_{\rm a}(N_{\rm a}/2)\ \cdots\ h_{\rm a}(N_{\rm a}-1)]^{\rm T}, & \text{if } N_{\rm a} \text{ is even;} \end{cases} \tag{2b}$$

$$\boldsymbol{c}_{\rm a}(\omega) = \begin{cases} [1\ \cos(M\omega)\ \cdots\ \cos[(N_{\rm a}-1)M\omega/2]]^{\rm T}, \\ \qquad \text{if } N_{\rm a} \text{ is odd;} \\ [\cos(M\omega/2)\ \cdots\ \cos[(N_{\rm a}-1)M\omega/2]]^{\rm T}, \\ \qquad \text{if } N_{\rm a} \text{ is even;} \end{cases} \tag{2c}$$

$$\boldsymbol{a}_{\rm ma} = \begin{cases} [h_{\rm ma}((N_{\rm ma}-1)/2)\ 2h_{\rm ma}((N_{\rm ma}+1)/2)\ \cdots \\ \quad 2h_{\rm ma}(N_{\rm ma}-1)]^{\rm T}, & \text{if } N_{\rm ma} \text{ is odd;} \\ 2[h_{\rm ma}(N_{\rm ma}/2)\ \cdots\ h_{\rm ma}(N_{\rm ma}-1)]^{\rm T}, \\ \qquad \text{if } N_{\rm ma} \text{ is even;} \end{cases} \tag{2d}$$

$$\boldsymbol{c}_{\rm ma}(\omega) = \begin{cases} [1\ \cos\omega\ \cdots\ \cos[(N_{\rm ma}-1)\omega/2]]^{\rm T}, \\ \qquad \text{if } N_{\rm ma} \text{ is odd;} \\ [\cos(\omega/2)\ \cdots\ \cos[(N_{\rm ma}-1)\omega/2]]^{\rm T}, \\ \qquad \text{if } N_{\rm ma} \text{ is even;} \end{cases} \tag{2e}$$

$$\boldsymbol{a}_{\rm mc} = \begin{cases} [h_{\rm mc}((N_{\rm mc}-1)/2)\ 2h_{\rm mc}((N_{\rm mc}+1)/2)\ \cdots \\ \quad 2h_{\rm mc}(N_{\rm mc}-1)]^{\rm T}, & \text{if } N_{\rm mc} \text{ is odd;} \\ 2[h_{\rm mc}(N_{\rm mc}/2)\ \cdots\ h_{\rm mc}(N_{\rm mc}-1)]^{\rm T}, \\ \qquad \text{if } N_{\rm mc} \text{ is even;} \end{cases} \tag{2f}$$

$$\boldsymbol{c}_{\rm mc}(\omega) = \begin{cases} [1\ \cos\omega\ \cdots\ \cos[(N_{\rm mc}-1)\omega/2]]^{\rm T}, \\ \qquad \text{if } N_{\rm mc} \text{ is odd;} \\ [\cos(\omega/2)\ \cdots\ \cos[(N_{\rm mc}-1)\omega/2]]^{\rm T}, \\ \qquad \text{if } N_{\rm mc} \text{ is even.} \end{cases} \tag{2g}$$

Consider the design of a low-pass filter as an example. Given M, the normalized passband edge $\omega_{\rm p}$ and the stopband edge $\omega_{\rm a}$, an initial design of subfilters $H_{\rm a}(z)$, $H_{\rm ma}(z)$, and $H_{\rm mc}(z)$ can be obtained using a standard method, such as Remez, WLS, or the BPNN algorithm as discussed in Section 3. The passband and stopband edges for $H_{\rm a}(z)$, $H_{\rm ma}(z)$, and $H_{\rm mc}(z)$ are determined as follows[13].

1) For $H_{\rm a}(z)$, the passband edge θ and stopband edge ϕ are given by either (3) or (4) depending on which set of $\{\theta, \phi\}$ satisfies $0 < \theta < \phi < \pi$.

$$\theta = \omega_{\rm p}M - 2m\pi; \tag{3a}$$

$$\phi = \omega_{\rm a}M - 2m\pi; \tag{3b}$$

$$m = \lfloor \omega_{\rm p}M/2\pi \rfloor; \tag{3c}$$

$$\theta = 2m\pi - \omega_{\rm a}M; \tag{4a}$$

$$\phi = 2m\pi - \omega_{\rm p}M; \tag{4b}$$

$$m = \lceil \omega_{\rm a}M/2\pi \rceil; \tag{4c}$$

where $\lfloor x \rfloor$ denotes the largest integer less than x, and $\lceil x \rceil$ denotes the smallest integer larger than x.

2) If (3) is used to determine the values of θ and ϕ, then the passband and stopband edges of $H_{\rm ma}(z)$ are given by $(2m\pi+\theta)/M$ and $[(2(m+1)\pi-\phi]/M$, respectively, and the passband and stopband edges of $H_{\rm mc}(z)$ are given by $(2m\pi-\theta)/M$ and $(2m\pi+\phi)/M$, respectively.

3) If (4) is used to determine the values of θ and ϕ, then the passband and stopband edges of $H_{\rm ma}(z)$ are given by $[(2(m-1)\pi+\phi]/M$ and $(2m\pi-\theta)/M$, respectively, and the passband and stopband edges of $H_{\rm mc}(z)$ are given by $(2m\pi-\phi)/M$ and $(2m\pi+\theta)/M$, respectively.

3 Neural Network Design Approach

The optimization process is done on a dense grid of frequencies ω_l, where $l = 1, 2, \ldots, L$. Using (2a), the vector of $H(\omega)$ evaluated on the set of ω_l, $l = 1, \ldots, L$, can be expressed as

$$\begin{aligned}\boldsymbol{H} &= (\boldsymbol{a}_{\rm a}^{\rm T}\boldsymbol{C}_{\rm a}).*(\boldsymbol{a}_{\rm ma}^{\rm T}\boldsymbol{C}_{\rm ma} - \boldsymbol{a}_{\rm mc}^{\rm T}\boldsymbol{C}_{\rm mc}) + \boldsymbol{a}_{\rm mc}^{\rm T}\boldsymbol{C}_{\rm mc} \\ &= \boldsymbol{H}_{\rm a}.*(\boldsymbol{H}_{\rm ma} - \boldsymbol{H}_{\rm mc}) + \boldsymbol{H}_{\rm mc},\end{aligned} \tag{5a}$$

where, ".∗" is matrix element group multiply operation in MATLAB, i.e., $\boldsymbol{A}.*\boldsymbol{B} = [A_{ij}B_{ij}]_{N\times M}$, and

$$\boldsymbol{C}_{\rm a} = [\boldsymbol{c}_{\rm a}(\omega_1), \boldsymbol{c}_{\rm a}(\omega_2), \ldots, \boldsymbol{c}_{\rm a}(\omega_L)]; \tag{5b}$$

$$\boldsymbol{C}_{\rm ma} = [\boldsymbol{c}_{\rm ma}(\omega_1), \boldsymbol{c}_{\rm ma}(\omega_2), \ldots, \boldsymbol{c}_{\rm ma}(\omega_L)]; \tag{5c}$$

$$\boldsymbol{C}_{\rm mc} = [\boldsymbol{c}_{\rm mc}(\omega_1), \boldsymbol{c}_{\rm mc}(\omega_2), \ldots, \boldsymbol{c}_{\rm mc}(\omega_L)]. \tag{5d}$$

Define the error function

$$\boldsymbol{e} = \boldsymbol{B}.*\boldsymbol{W}.*(\boldsymbol{M}_{\rm d} - \boldsymbol{H}) \tag{6}$$

where $\boldsymbol{M}_{\rm d}$ is the vector of desired responses evaluated on ω_l, $l = 1, 2, \ldots, L$, $\boldsymbol{B}$ and $\boldsymbol{W}$ are the frequency weighting function vectors which are defined in (25) and (26), respectively. The optimization problem is to minimize the objective function

$$J = \frac{1}{2}\sum_{l=0}^{L} e^2(l) = \frac{1}{2}\|\boldsymbol{e}\|_2^2. \tag{7}$$

3.1 Neural Network Algorithm

The main difficulty in minimizing the objective function (7) is its high degree of nonlinearity with respect to the coefficients of the subfilters. By carefully examining of the objective function (7), it can be seen that the coefficient set $\{\boldsymbol{a}_{\rm a}, \boldsymbol{a}_{\rm ma}, \boldsymbol{a}_{\rm mc}\}$ can be divided into two subsets, namely $\{\boldsymbol{a}_{\rm a}\}$ and $\{\boldsymbol{a}_{\rm ma}, \boldsymbol{a}_{\rm mc}\}$. Each subset contains the coefficients of one or two subfilters which are connected in parallel. Consequently, the frequency-response magnitude of the overall filter is linear with respect to the coefficients of any one of these subsets. For this, let us first define the following two neural network linear optimization subproblems.

Problem (P_1): the coefficients $\boldsymbol{a}_{\rm ma}$ and $\boldsymbol{a}_{\rm mc}$ of the objective function (7) are taken as fixed. Let the corresponding new objective function (7) be denoted as $\in_1 (\boldsymbol{a}_{\rm a}, \eta|\boldsymbol{B}, \boldsymbol{a}_{\rm ma}, \boldsymbol{a}_{\rm mc})$, where η is the learning rate of coefficient vector $\boldsymbol{a}_{\rm a}$.

Problem (P_2): the coefficients $\boldsymbol{a}_{\rm a}$ of the objective function (7) are taken as fixed. Let the corresponding new objective function (7) be denoted as $\in_2 (\boldsymbol{a}_{\rm ma}, \boldsymbol{a}_{\rm mc}, \eta_1|\boldsymbol{B}, \boldsymbol{a}_{\rm a})$, where η_1 is the learning rate of coefficient vectors $\boldsymbol{a}_{\rm ma}$ and $\boldsymbol{a}_{\rm mc}$.

Choosing a positive integer m, and a small positive ε, the proposed neural network optimization process is then described as follows.

Step 1) Initial Design: For a given set of M, $N_{\rm a}$, $N_{\rm ma}$, $N_{\rm mc}$, $\omega_{\rm p}$ and $\omega_{\rm a}$, an initial design can be obtained by using a simple standard method, such as Remez or WLS or NN algorithm as discussed in this section. (In this study, we use the NN algorithm to design these filters.) The coefficients of $H_{\rm a}(z)$, $H_{\rm ma}(z)$ and $H_{\rm mc}(z)$ are used to form the initial parameter vectors of $\boldsymbol{a}_{\rm a}$, $\boldsymbol{a}_{\rm ma}$ and $\boldsymbol{a}_{\rm mc}$, respectively. Set the initial weighting function $B_0(\omega_l) = 1$, $l = 1, 2, \ldots, L$, and iteration number, $k = 0$. Set $i = 1$.

Step 2) Minimize $\in_1 (\boldsymbol{a}_{\rm a}, \eta|\boldsymbol{B}_k, \boldsymbol{a}_{{\rm ma}(k)}, \boldsymbol{a}_{{\rm mc}(k)})$ with respect to the coefficients $\boldsymbol{a}_{\rm a}$. Denote the optimal coefficients obtained as $\boldsymbol{a}_{{\rm a}(k)}$.

Step 3) Minimize $\in_2 (\boldsymbol{a}_{\rm ma}, \boldsymbol{a}_{\rm mc}, \eta_1|\boldsymbol{B}_k, \boldsymbol{a}_{{\rm a}(k)})$ with respect to the coefficients $\boldsymbol{a}_{\rm ma}$ and $\boldsymbol{a}_{\rm mc}$. Denote the optimal coefficients obtained as $\boldsymbol{a}_{{\rm ma}(k)}$ and $\boldsymbol{a}_{{\rm mc}(k)}$. Set $i = i + 1$. If $i = m$, go to Step 4); otherwise, go to Step 2).

Step 4) Calculate the objective function (7). If $J < \varepsilon$, stop; otherwise, update weighting vector $\boldsymbol{B}$. Set $k = k + 1$, $i = 1$ and go to Step 2).

In the above, the values of learning rate η and η_1 are selected according to Theorems 1 and 2, respectively, in Subsection 3.1.1, and weighting vector $\boldsymbol{B}$ is defined in (27). In Step 4) of the above algorithm, weighting vector $\boldsymbol{B}$ is updated by every m iteration. From our extensive simulations, we find that it is sufficient to choose m to be between 3 and 5 (in all the following examples, m is chosen to be 5).

3.1.1 Neural Network Solutions to Problems (P_1) and (P_2)

To solve Problem (P_1), the coefficients $\boldsymbol{a}_{\rm ma}$ and $\boldsymbol{a}_{\rm mc}$ of (5a) are taken as fixed, i.e., the magnitude response vectors $\boldsymbol{H}_{\rm ma}$ and $\boldsymbol{H}_{\rm mc}$ of subfilters $H_{\rm ma}(z)$ and $H_{\rm mc}(z)$ are also taken as fixed. According to this equation, we establish a BBPNN model as shown in Fig.2. There, three layers are considered: input, hidden, and output lay. The frequency grid vector $\boldsymbol{\omega}$ and the magnitude response vectors $\boldsymbol{H}_{\rm ma}$ and $\boldsymbol{H}_{\rm mc}$ are all considered as the neural network input, and the weight of each input neuron is 1. The activation function of the hidden neuron is composed of all the elements of the cosine matrix $\boldsymbol{C}_{\rm a}$, and the weight of the activation function matrix is vector $\boldsymbol{a}_{\rm a}^{\rm T}$. The magnitude response vector $\boldsymbol{H}$ of the overall filter $H(z)$ is considered as the output of the neural network. According to the steepest decent algorithm, the coefficient vector $\boldsymbol{a}_{\rm a}$ is recursively updated as follows.

$$\begin{aligned}\boldsymbol{a}_{{\rm a}(i+1)} &= \boldsymbol{a}_{{\rm a}(i)} - \eta\frac{\partial J}{\partial a_{{\rm a}(i)}}\\ &= \boldsymbol{a}_{{\rm a}(i)} + \eta\boldsymbol{C}_{\rm a}[\boldsymbol{W}^{\rm T}.*\boldsymbol{B}^{\rm T}.*\boldsymbol{e}_i^{\rm T}.*(\boldsymbol{a}_{\rm ma}^{\rm T}\boldsymbol{C}_{\rm ma}\\ &\quad - \boldsymbol{a}_{\rm mc}^{\rm T}\boldsymbol{C}_{\rm mc})^{\rm T}],\end{aligned} \tag{8}$$

where $\boldsymbol{a}_{{\rm a}(i)}$ is the value of $\boldsymbol{a}_{\rm a}$ for the i-th iteration, and $\eta > 0$ is the learning rate. Define $\max(\boldsymbol{X})$ as the largest element in matrix $\boldsymbol{X}$. We can prove the convergence of the neural network algorithm.

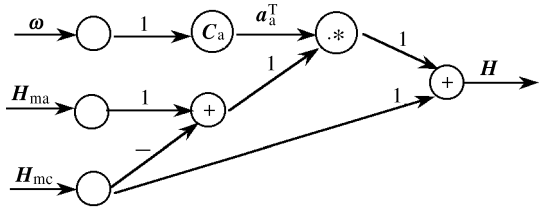

Fig.2. Neural network model.

Theorem 1. *If the learning rate satisfies* $\eta < \frac{2}{\mu^2(\max(\boldsymbol{B}))^2\|\boldsymbol{C}_{\rm a}\|^2}$, *where* $\mu = \max\{\boldsymbol{H}_{\rm ma}, \boldsymbol{H}_{\rm mc}\}$, *the algorithm is convergent to its global minimum.*

Proof. Define (7) as a Lyapunov function. From (5a), we have

$$\begin{aligned}\mathrm{diag}(\boldsymbol{H}_i) &= \mathrm{diag}\{(\boldsymbol{a}_{{\rm a}(i)}^{\rm T}\boldsymbol{C}_{\rm a}).*\\ &\quad (\boldsymbol{a}_{\rm ma}^{\rm T}\boldsymbol{C}_{\rm ma} - \boldsymbol{a}_{\rm mc}^{\rm T}\boldsymbol{C}_{\rm mc}) + \boldsymbol{a}_{\rm mc}^{\rm T}\boldsymbol{C}_{\rm mc}\}\\ &= \boldsymbol{A}_{{\rm a}(i)}(\boldsymbol{A}_{\rm ma} - \boldsymbol{A}_{\rm mc}) + \boldsymbol{A}_{\rm mc},\end{aligned} \tag{9a}$$

where $\mathrm{diag}(\boldsymbol{V})$ means creating a diagonal matrix with the elements of vector $\boldsymbol{V}$ on the main diagonal, and

$$\boldsymbol{A}_{{\rm a}(i)} = \mathrm{diag}[\boldsymbol{a}_{{\rm a}(i)}^{\rm T}\boldsymbol{C}_{\rm a}] = \mathrm{diag}(\boldsymbol{H}_{{\rm a}(i)}); \tag{9b}$$

$$\boldsymbol{A}_{\rm ma} = \mathrm{diag}[\boldsymbol{a}_{\rm ma}^{\rm T}\boldsymbol{C}_{\rm ma}] = \mathrm{diag}(\boldsymbol{H}_{\rm ma}); \tag{9c}$$

$$\boldsymbol{A}_{\rm mc} = \mathrm{diag}[\boldsymbol{a}_{\rm mc}^{\rm T}\boldsymbol{C}_{\rm mc}] = \mathrm{diag}(\boldsymbol{H}_{\rm mc}). \tag{9d}$$

Now define

$$\boldsymbol{B}_1 = \mathrm{diag}(\boldsymbol{B}); \tag{10}$$

$$\boldsymbol{W}_1 = \mathrm{diag}(\boldsymbol{W}); \tag{11}$$

then (8) can be rewritten as

$$\begin{aligned}\Delta\boldsymbol{a}_{{\rm a}(i)} &= \boldsymbol{a}_{{\rm a}(i+1)} - \boldsymbol{a}_{{\rm a}(i)}\\ &= \eta\boldsymbol{C}_{\rm a}\boldsymbol{B}_1\boldsymbol{W}_1(\boldsymbol{A}_{\rm ma} - \boldsymbol{A}_{\rm mc})\boldsymbol{e}_i^{\rm T}\\ &= \eta\boldsymbol{X}_{\rm a}\boldsymbol{e}_i^{\rm T},\end{aligned} \tag{12}$$

where $\boldsymbol{X}_{\rm a} = \boldsymbol{C}_{\rm a}\boldsymbol{B}_1\boldsymbol{W}_1(\boldsymbol{A}_{\rm ma} - \boldsymbol{A}_{\rm mc})$. Then we have

$$\frac{\partial\boldsymbol{e}}{\partial\boldsymbol{a}_{{\rm a}(i)}} = -\boldsymbol{X}_a; \tag{13}$$

$$\Delta\boldsymbol{e}_i = (\Delta\boldsymbol{a}_{{\rm a}(i)})^{\rm T}\frac{\partial\boldsymbol{e}}{\partial\boldsymbol{a}_{{\rm a}(i)}} = -\eta\boldsymbol{e}_i\boldsymbol{X}_{\rm a}^{\rm T}\boldsymbol{X}_{\rm a}; \tag{14}$$

and then

$$\begin{aligned}\Delta J_i &= \|\boldsymbol{e}_i - \eta\boldsymbol{e}_i\boldsymbol{X}_{\rm a}^{\rm T}\boldsymbol{X}_{\rm a}\|^2 - \|\boldsymbol{e}_i\|^2\\ &\leqslant \|\boldsymbol{I} - \eta\boldsymbol{X}_{\rm a}^{\rm T}\boldsymbol{X}_{\rm a}\|^2\|\boldsymbol{e}_i\|^2 - \|\boldsymbol{e}_i\|^2\\ &= (1 - 2\eta\|\boldsymbol{X}_{\rm a}^{\rm T}\boldsymbol{X}_{\rm a}\| + \eta^2\|\boldsymbol{X}_{\rm a}^{\rm T}\boldsymbol{X}_{\rm a}\|^2)\|\boldsymbol{e}_i\|^2 - \|\boldsymbol{e}_i\|^2\\ &= \eta\|\boldsymbol{e}_i\|^2\|\boldsymbol{X}_{\rm a}^{\rm T}\boldsymbol{X}_{\rm a}\| \times (\eta\|\boldsymbol{X}_{\rm a}^{\rm T}\boldsymbol{X}_{\rm a}\| - 2)\\ &\leqslant \eta\|\boldsymbol{e}_i\|^2\|\boldsymbol{X}_{\rm a}^{\rm T}\boldsymbol{X}_{\rm a}\|[\eta(\|\boldsymbol{X}_{\rm a}\|^2) - 2].\end{aligned} \tag{15}$$

To simplify the above equation, we define $\mu = \max\{\boldsymbol{H}_{\rm ma}, \boldsymbol{H}_{\rm mc}\}$, and set $\max(\boldsymbol{W}) = 1$. Since

$$\begin{aligned}\|\boldsymbol{X}_{\rm a}\| &= \|\boldsymbol{C}_{\rm a}\boldsymbol{B}_1\boldsymbol{W}_1(\boldsymbol{A}_{\rm ma} - \boldsymbol{A}_{\rm mc})\|\\ &\leqslant \|\boldsymbol{B}_1\|\|\boldsymbol{W}_1\|\|\boldsymbol{A}_{\rm ma} - \boldsymbol{A}_{\rm mc}\|\|\boldsymbol{C}_{\rm a}\|,\end{aligned} \tag{16}$$

then

$$\|\boldsymbol{X}_{\rm a}\| \leqslant \mu\max(\boldsymbol{B}_1)\|\boldsymbol{C}_{\rm a}\| = \mu\max(\boldsymbol{B})\|\boldsymbol{C}_{\rm a}\|; \tag{17}$$

$$\Delta J_i \leqslant \eta\|\boldsymbol{e}_i\|^2\|\boldsymbol{X}_{\rm a}^{\rm T}\boldsymbol{X}_{\rm a}\| \times [\eta\mu^2(\max(\boldsymbol{B}))^2\|\boldsymbol{C}_{\rm a}\|^2 - 2]. \tag{18}$$

If

$$\eta < \frac{2}{\mu^2(\max(\boldsymbol{B}))^2\|\boldsymbol{C}_{\rm a}\|^2}, \tag{19}$$

then

$$\Delta J_i \leqslant 0, \tag{20}$$

and if

$$\Delta J_i = 0, \tag{21}$$

we have

$$\boldsymbol{e}_i = 0; \tag{22a}$$

$$\Delta\boldsymbol{a}_{{\rm a}(i)} = 0; \tag{22b}$$

$$J_i = 0. \tag{22c}$$

Therefore, if $\eta < \frac{2}{\mu^2(\max(\boldsymbol{B}))^2\|\boldsymbol{C}_{\rm a}\|^2}$, the neural network algorithm will converge asymptotically to its global minimum. The theorem is proved. □

The theorem means that the network (8) is stable and the energy function (7) will converge to its global minimum as the coefficients $\boldsymbol{a}_{\rm ma}$ and $\boldsymbol{a}_{\rm mc}$ of (5a) are taken as fixed.

Similarly, for Problem (P_2), the coefficient $\boldsymbol{a}_{\rm a}$ of (5a) is taken as fixed. A similar BBPNN model can also be established. The coefficients $\boldsymbol{a}_{\rm ma}$ and $\boldsymbol{a}_{\rm mc}$ can be recursively updated using

$$\begin{aligned}\boldsymbol{a}_{{\rm ma}(i+1)} =& \boldsymbol{a}_{{\rm ma}(i)} + \eta_1 \boldsymbol{C}_{\rm ma}(\boldsymbol{W}^{\rm T} .* \boldsymbol{B}^{\rm T} \\ & .* \boldsymbol{e}_i^{\rm T} .* [\boldsymbol{a}_{\rm a}^{\rm T}\boldsymbol{C}_{\rm a}]^{\rm T}); \qquad (23a)\\ \boldsymbol{a}_{{\rm mc}(i+1)} =& \boldsymbol{a}_{{\rm mc}(i)} + \eta_1 \boldsymbol{C}_{\rm mc}(\boldsymbol{W}^{\rm T} .* \boldsymbol{B}^{\rm T} \\ & .* \boldsymbol{e}_i^{\rm T} .* [1 - \boldsymbol{a}_{\rm a}^{\rm T}\boldsymbol{C}_{\rm a}]^{\rm T}); \qquad (23b)\end{aligned}$$

where $\eta_1 > 0$ is the learning rate. Define (7) as a new Lyapunov function. We can also prove the following convergence theorem.

Theorem 2. *If the learning rate satisfies* $\eta < \frac{2}{\nu^2(\max(\boldsymbol{B}))^2(\|\boldsymbol{C}_{\rm ma}\|^2+\|\boldsymbol{C}_{\rm mc}\|^2)}$, *where* $\nu = \max(\boldsymbol{H}_{\rm a})$, *the algorithm is convergent to its global minimum.*

This means we can use (23) to obtain optimal coefficients $\boldsymbol{a}_{\rm ma}$ and $\boldsymbol{a}_{\rm mc}$ as the coefficient $\boldsymbol{a}_{\rm a}$ of (5a) is taken as fixed.

3.1.2 Design Guidelines

We shall use the following design guidelines to illustrate our technique.

1) Desired Frequency Response and Weighting Function $\boldsymbol{W}$: Consider the case of designing a lowpass FRM filter where each delay in $H_{\rm a}(z)$ is replaced with M delays. The passband edge and stopband edge are $\omega_{\rm p}$ and $\omega_{\rm a}$, respectively. The desired response $M_{\rm d}(\omega_l)$ in this case is

$$M_{\rm d}(\omega_l) = \begin{cases} 1, & \text{for } 0 \leqslant \omega_l \leqslant \omega_{\rm p}; \\ 0, & \text{for } \omega_{\rm a} \leqslant \omega_l \leqslant \pi. \end{cases} \qquad (24)$$

The weighting function is

$$W(\omega_l) = \begin{cases} 1, & \text{for } 0 \leqslant \omega_l \leqslant \omega_{\rm p}; \\ \delta_{\rm p}/\delta_{\rm s}, & \text{for } \omega_{\rm a} \leqslant \omega_l \leqslant \pi; \end{cases} \qquad (25)$$

where $\delta_{\rm p}$ and $\delta_{\rm s}$ are the desired passband and stopband ripples, respectively.

2) Weighting Function $\boldsymbol{B}$: Set initial weighting function $\boldsymbol{B}$ as

$$B(\omega_l) = \begin{cases} 1, & \text{for } 0 \leqslant \omega_l \leqslant \omega_{\rm p}; \\ 1, & \text{for } \omega_{\rm a} \leqslant \omega_l \leqslant \pi. \end{cases} \qquad (26)$$

To design equiripple or quasi-equiripple FIR filters, the weighting function $B(\omega_l)$ needs to be updated as the following (also see [14]):

$$B_{k+1}(\omega_l) = B_k(\omega_l)\frac{|W(\omega_l)(M_{\rm d}(\omega_l) - H_k(\omega_l))|}{\sum_l |e_k(\omega_l)|}. \qquad (27)$$

In order for $B_{k+1}(\omega_l)$ to avoid getting too close to zero, it is necessary to be specified a lower bound, r. Our extensive numerical experience indicates that, for numerical stability, r should be close to 0.001.

3) Placement of Grid Points: Dense grid points are obtained in $[0, \omega_{\rm p}] \cup [\omega_{\rm a}, \pi]$. Our designing has indicated that relatively denser grid points should be placed in the regions near the band edges in both passband and stopband so as to avoid unnecessarily using a large number of total grid points. The general practice is to have M times denser grid points in the frequency closer to the bandedge than that of the others, where M is the number of zeros inserted in between two adjacent coefficients in FRM. For multiple-stage FRM techniques, the grid frequency will be $M_1 \times M_2 \times \cdots$ times accordingly.

3.2 Design Example

Example 1. The design is a linear-phase low-pass FRM filter with the same design parameters as the first example in [4, 11, 13], i.e., $\omega_{\rm p} = 0.6\pi$, $\omega_{\rm a} = 0.61\pi$, $N_{\rm a} = 45$, $N_{\rm ma} = 41$, $N_{\rm mc} = 33$, and $M = 9$. Set $\delta_{\rm p}/\delta_{\rm s} = 1.1$, $L = 900$. After 1500 training iterations (the computer used 8.9 seconds on a CPU of Pentium4), the algorithm converges to an FRM filter with the amplitude responses of its sub-filters $H_{\rm a}(z^M)$, $H_{\rm ma}(z)$, and $H_{\rm mc}(z)$ shown in Figs. 3(a) and 3(b), respectively, and the amplitude response of the FRM filter and its passband ripples shown in Figs. 3(c) and 3(d), respectively. The maximum passband ripple is found to be 0.0583dB and the minimum stopband attenuation is 42.64dB. In [4, 11], the passband ripple and stopband attenuation are 0.0896dB and 40.96dB, respectively whereas those in [13] are 0.0674dB and 42.25dB, respectively.

Example 2. This is a linear-phase low-pass FRM filter with the same design parameters as the first example in [12–14], i.e., $\omega_{\rm p} = 0.4\pi$, $\omega_{\rm a} = 0.402\pi$, and $M = 21$. Set $N_{\rm a} = 99$, $N_{\rm ma} = 71$, $N_{\rm mc} = 87$. Define $\delta_{\rm p}/\delta_{\rm s} = 10$, $L = 1900$. After 3000 training iterations, the algorithm converges to an FRM filter with the amplitude responses of its subfilters $H_{\rm a}(z^M)$, $H_{\rm ma}(z)$, and $H_{\rm mc}(z)$ shown in Figs. 4(a) and 4(b), respectively, and the amplitude response of the FRM filter and its passband ripples shown in Figs.4(c) and 4(d), respectively. The maximum passband ripple is found to be 0.0665dB and the minimum stopband attenuation 61.64dB, and the group delay $D = 1072$. For the purpose of comparison, in [12–4], $N_{\rm a} = 123$, $N_{\rm ma} = 56$, $N_{\rm mc} = 78$, and the passband ripple and stopband attenuation of the design in [12, 14] are 0.0864dB and 60dB, respectively, and in

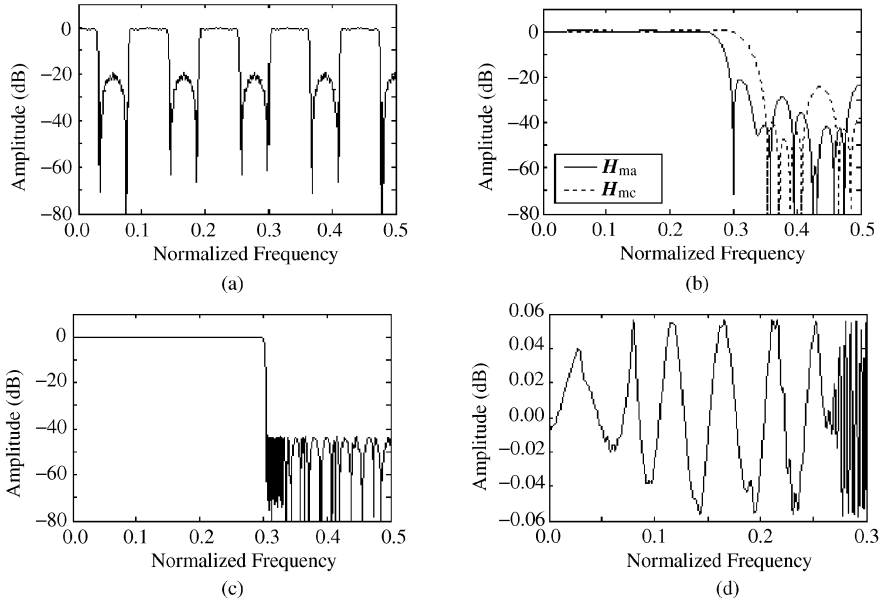

Fig.3. Amplitude responses. (a) Prototype filter $H_a(z^9)$. (b) Masking filters $H_{ma}(z)$ and $H_{mc}(z)$. (c) FRM filter. (d) Passband ripples of the FRM filter.

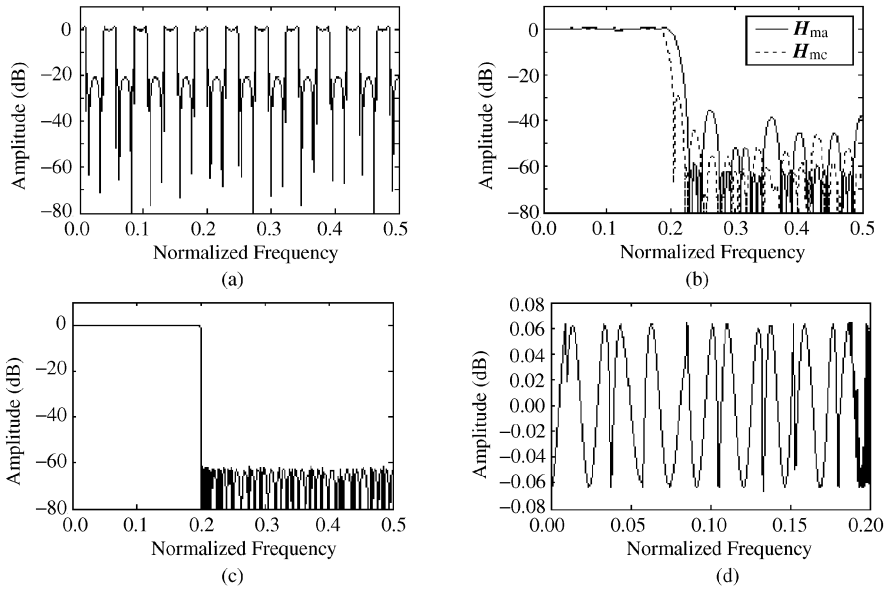

Fig.4. Amplitude responses. (a) Prototype filter $H_a(z^{21})$. (b) Masking filters $H_{ma}(z)$ and $H_{mc}(z)$. (c) FRM filter. (d) Passband ripples of the FRM filter.

[13] are 0.0855dB and 60.93dB, respectively, and the group delays are $D = 1319.5$ in [12–14]. Therefore, our proposed approach offers better performance than the proposed two-step design approach in [12], the SDP method in [13] and the WLS method in [14].

4 Multistage FRM Filter Design

4.1 Design Approach

The algorithm in Section 3 also applies to multistage FRM filters. For the sake of notation simplicity, in what follows we focus our attention on the two-stage case shown in Fig.5. The proposed approach can be extended for the design of FRM filters with more than two stages.

Since the subfilters involved have linear phase responses, they will be treated as zero-phase filters and the frequency response of the two-stage FRM filter can be expressed as

$$\boldsymbol{H} = \boldsymbol{H}_{\rm a}^{(1)}.*(\boldsymbol{a}_{\rm 1ma}^{\rm T}\boldsymbol{C}_{\rm 1ma} - \boldsymbol{a}_{\rm 1mc}^{\rm T}\boldsymbol{C}_{\rm 1mc}) + \boldsymbol{a}_{\rm 1mc}^{\rm T}\boldsymbol{C}_{\rm 1mc}, \tag{28a}$$

where

$$\boldsymbol{H}_{\rm a}^{(1)} = (\boldsymbol{a}_{\rm 2a}^{\rm T}\boldsymbol{C}_{\rm 2a}).*(\boldsymbol{a}_{\rm 2ma}^{\rm T}\boldsymbol{C}_{\rm 2ma} - \boldsymbol{a}_{\rm 2mc}^{\rm T}\boldsymbol{C}_{2mc}) + \boldsymbol{a}_{\rm 2mc}^{\rm T}\boldsymbol{C}_{\rm 2mc}. \tag{28b}$$

The vectors $\boldsymbol{a}_{\rm 2a}$, $\boldsymbol{a}_{j\rm ma}$ and $\boldsymbol{a}_{j\rm mc}$ $(j = 1, 2)$ in (28) are the coefficient vectors for filters $H_{\rm a}^{(2)}(z)$, $H_{\rm ma}^{(j)}(z)$ and $H_{\rm mc}^{(j)}(z)$, respectively, and are defined in a way similar to vectors $\boldsymbol{a}_{\rm a}$, $\boldsymbol{a}_{\rm ma}$ and $\boldsymbol{a}_{\rm mc}$ in (2), respectively. The cosine matrixes for the first-stage masking filters, namely $\boldsymbol{C}_{\rm 1ma}$ and $\boldsymbol{C}_{\rm 1mc}$, are defined in the same way as $\boldsymbol{C}_{\rm ma}$ and $\boldsymbol{C}_{\rm mc}$ in (5) and (2); and the cosine matrixes for the second-stage subfilters, i.e., $\boldsymbol{C}_{\rm 2a}$, $\boldsymbol{C}_{\rm 2ma}$ and $\boldsymbol{C}_{\rm 2mc}$ are defined in a way similar to $\boldsymbol{C}_{\rm a}$, $\boldsymbol{C}_{\rm ma}$ and $\boldsymbol{C}_{\rm mc}$ in (5) and (2) except that each ω is replaced with $M\omega$. The group delay of the FRM filter is given in [13]

$$D = \frac{(N_{\rm 2a} - 1)M^2}{2} + d_2 M + d_1, \tag{29}$$

where $N_{\rm 2a}$ is the length of $H_{\rm a}^{(2)}(z)$ and $d_j = \max\{(N_{j\rm ma} - 1)/2,\ (N_{j\rm mc} - 1)/2\}$ for $j = 1, 2$ with $N_{j\rm ma}$ and $N_{j\rm mc}$ being the lengths of the masking filters $H_{\rm ma}^{(j)}(z)$ and $H_{\rm mc}^{(j)}(z)$, respectively. Define new error function $\boldsymbol{e}$ and objective function J in a way similar to (6) and (7), respectively. By examination of the objective function (7), it can be seen that the coefficient set $\{\boldsymbol{a}_{\rm 2a}, \boldsymbol{a}_{\rm 2ma}, \boldsymbol{a}_{\rm 2mc}, \boldsymbol{a}_{\rm 1ma}, \boldsymbol{a}_{\rm 1mc}\}$ can be divided into three subsets, namely $\{\boldsymbol{a}_{\rm 2a}\}$, $\{\boldsymbol{a}_{\rm 2ma}, \boldsymbol{a}_{\rm 2mc}\}$ and $\{\boldsymbol{a}_{\rm 1ma}, \boldsymbol{a}_{\rm 1mc}\}$. Each subset also contains the coefficients of one or two subfilters which are connected in parallel. Consequently, the frequency-response magnitude of the overall filter is linear with respect to the coefficients of any one of these subsets. For this, we first define the following three neural network linear optimization subproblems.

Problems (P_1), (P_2) and (P_3): the coefficient sets $\{\boldsymbol{a}_{\rm 2ma}, \boldsymbol{a}_{\rm 2mc}, \boldsymbol{a}_{\rm 1ma}, \boldsymbol{a}_{\rm 1mc}\}$, $\{\boldsymbol{a}_{\rm 2a}, \boldsymbol{a}_{\rm 1ma}, \boldsymbol{a}_{\rm 1mc}\}$ and $\{\boldsymbol{a}_{\rm 2a}, \boldsymbol{a}_{\rm 2ma}, \boldsymbol{a}_{\rm 2mc}\}$ of the new objective function (7) are taken as fixed as Problems (P_1), (P_2) and (P_3), respectively. The corresponding objective function (7) for Problems (P_1), (P_2) and (P_3) are denoted by

$$\begin{aligned}
&\in_1 (\boldsymbol{a}_{\rm 2a}, \eta | \boldsymbol{B}, \boldsymbol{a}_{\rm 2ma}, \boldsymbol{a}_{\rm 2mc}, \boldsymbol{a}_{\rm 1ma}, \boldsymbol{a}_{\rm 1mc});\\
&\in_2 (\boldsymbol{a}_{\rm 2ma}, \boldsymbol{a}_{\rm 2mc}, \eta_1 | \boldsymbol{B}, \boldsymbol{a}_{\rm 2a}, \boldsymbol{a}_{\rm 1ma}, \boldsymbol{a}_{\rm 1mc});\\
&\in_3 (\boldsymbol{a}_{\rm 1ma}, \boldsymbol{a}_{\rm mc}, \eta_2 | \boldsymbol{B}, \boldsymbol{a}_{\rm 2a}, \boldsymbol{a}_{\rm 2ma}, \boldsymbol{a}_{\rm 2mc});
\end{aligned}$$

respectively, where η, η_1 and η_2 are the learning rates of $\boldsymbol{a}_{2a}$, $\boldsymbol{a}_{\rm 2ma}$ and $\boldsymbol{a}_{\rm 2mc}$, and $\boldsymbol{a}_{\rm 1ma}$ and $\boldsymbol{a}_{\rm 1mc}$, respectively.

Choose a positive integer m, and a small positive ε. The proposed neural network optimization process is then described as follows.

Step 1) Initial Design: Use parameters M, $N_{\rm 1ma}$, $N_{\rm 1mc}$, $\omega_{\rm p}$ and $\omega_{\rm a}$ to obtain an initial design of $H_{\rm ma}^{(1)}(z)$ and $H_{\rm mc}^{(1)}(z)$. Use parameters M, $\omega_{\rm p}$ and $\omega_{\rm a}$ to obtain the values of θ and ϕ as the passband and stopband edges for $H_{\rm a}^{(1)}(z)$. Let $\hat{\omega}_{\rm p} = \theta$ and $\hat{\omega}_{\rm a} = \phi$. Use parameters M, $N_{\rm 2a}$, $N_{\rm 2ma}$, $N_{\rm 2mc}$, $\hat{\omega}_{\rm p}$ and $\hat{\omega}_{\rm a}$ to obtain an initial design of $H_{\rm a}^{(2)}(z)$, $H_{\rm ma}^{(2)}(z)$ and $H_{\rm mc}^{(2)}(z)$. The coefficients of subfilters $H_{\rm a}^{(2)}(z)$, $H_{\rm ma}^{(2)}(z)$, $H_{\rm mc}^{(2)}(z)$, $H_{\rm ma}^{(1)}(z)$ and $H_{\rm mc}^{(1)}(z)$ are now used to form the initial parameter vectors of $\boldsymbol{a}_{\rm 2a}$, $\boldsymbol{a}_{\rm 2ma}$, $\boldsymbol{a}_{\rm 2mc}$, $\boldsymbol{a}_{\rm 1ma}$ and $\boldsymbol{a}_{\rm 1mc}$, respectively. Set the initial weighting function $B_0(\omega_l) = 1$, $l = 1, 2, \ldots, L$, and iteration number, $k = 0$. Set $i = 1$.

Step 2) Minimize $\in_1$ $(\boldsymbol{a}_{\rm 2a}, \eta | \boldsymbol{B}_k, \boldsymbol{a}_{\rm 2ma(k)}, \boldsymbol{a}_{\rm 2mc(k)}, \boldsymbol{a}_{\rm 1ma(k)}, \boldsymbol{a}_{\rm 2mc(k)})$ with respect to the coefficients $\boldsymbol{a}_{\rm 2a}$. Denote the optimal coefficients obtained as $\boldsymbol{a}_{\rm 2a(k)}$.

Step 3) Minimize $\in_2$ $(\boldsymbol{a}_{\rm 2ma}, \boldsymbol{a}_{\rm 2mc}, \eta_1 | \boldsymbol{B}_k, \boldsymbol{a}_{\rm 2a(k)}, \boldsymbol{a}_{\rm 1ma(k)}, \boldsymbol{a}_{\rm 1mc(k)})$ with respect to the coefficients $\boldsymbol{a}_{\rm 2ma}$ and $\boldsymbol{a}_{\rm 2mc}$. Denote the optimal coefficients obtained as $\boldsymbol{a}_{\rm 2ma(k)}$ and $\boldsymbol{a}_{\rm 2mc(k)}$.

Step 4) Minimize $\in_3$ $(\boldsymbol{a}_{\rm 1ma}, \boldsymbol{a}_{\rm 1mc}, \eta_2 | \boldsymbol{B}_k, \boldsymbol{a}_{\rm 2a(k)}, \boldsymbol{a}_{\rm 2ma(k)}, \boldsymbol{a}_{\rm 2mc(k)})$ with respect to the coefficients $\boldsymbol{a}_{\rm 1ma}$ and $\boldsymbol{a}_{\rm 1mc}$. Denote the optimal coefficients obtained as $\boldsymbol{a}_{\rm 1ma(k)}$ and $\boldsymbol{a}_{\rm 1mc(k)}$. Set $i = i + 1$. If $i = m$, go to Step 5); otherwise, go to Step 2).

Step 5) Calculate the objective function (7). If $J < \varepsilon$, stop; otherwise, update weighting vector $\boldsymbol{B}$. Set $k = k + 1$, $i = 1$ and go to Step 2).

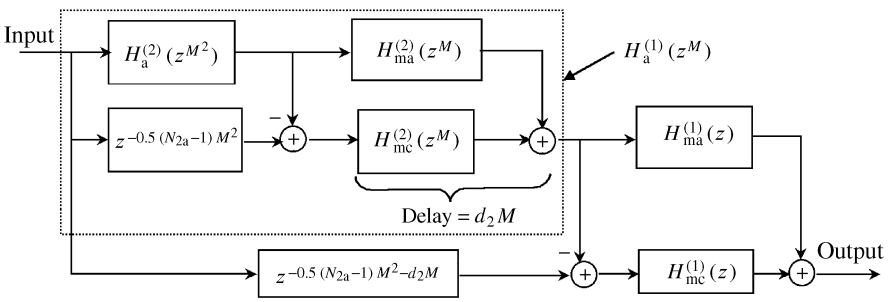

Fig.5. Two-stage FRM filter structure.

Similar to designing basic FRM filters, for solving Problems (P_1), (P_2) and (P_3), according to (28), we can establish three corresponding linear BBPNN models, which are similar to that in Fig.2, respectively. Then the values of learning rate η, η_1 and η_2 can be determined by using corresponding convergence theorems which can be presented similar to Theorem 1 or 2, and weighting vector $\boldsymbol{B}$ is also defined in (27). Consequently, for Problems (P_1), (P_2) and (P_3), $\boldsymbol{a}_{2\mathrm{a}}$, $\boldsymbol{a}_{2\mathrm{ma}}$ and $\boldsymbol{a}_{2\mathrm{mc}}$, and $\boldsymbol{a}_{1\mathrm{ma}}$ and $\boldsymbol{a}_{1\mathrm{mc}}$ are updated according to (30)$\sim$(32), respectively.

$$\boldsymbol{a}_{2\mathrm{a}(i+1)} = \boldsymbol{a}_{2\mathrm{a}(i)} + \eta \boldsymbol{C}_{2\mathrm{a}}(\boldsymbol{W}^{\mathrm{T}} .* \boldsymbol{B}^{\mathrm{T}} .* \boldsymbol{e}_i^{\mathrm{T}} .* \boldsymbol{z}_1^{\mathrm{T}} .* \boldsymbol{z}_2^{\mathrm{T}}); \tag{30}$$

$$\boldsymbol{a}_{2\mathrm{ma}(i+1)} = \boldsymbol{a}_{2\mathrm{ma}(i)} + \eta_1 \boldsymbol{C}_{2\mathrm{ma}}(\boldsymbol{W}^{\mathrm{T}} .* \boldsymbol{B}^{\mathrm{T}} .* \boldsymbol{e}_i^{\mathrm{T}} .* \boldsymbol{z}_1^{\mathrm{T}} .* \boldsymbol{z}_3^{\mathrm{T}}); \tag{31a}$$

$$\boldsymbol{a}_{2\mathrm{mc}(i+1)} = \boldsymbol{a}_{2\mathrm{mc}(i)} + \eta_1 \boldsymbol{C}_{2\mathrm{mc}}[\boldsymbol{W}^{\mathrm{T}} .* \boldsymbol{B}^{\mathrm{T}} .* \boldsymbol{e}_i^{\mathrm{T}} .* \boldsymbol{z}_1^{\mathrm{T}} .* (1 - \boldsymbol{z}_3)^{\mathrm{T}}]; \tag{31b}$$

$$\boldsymbol{a}_{1\mathrm{ma}(i+1)} = \boldsymbol{a}_{1\mathrm{ma}(i)} + \eta_2 \boldsymbol{C}_{1\mathrm{ma}}(\boldsymbol{W}^{\mathrm{T}} .* \boldsymbol{B}^{\mathrm{T}} .* \boldsymbol{e}_i^{\mathrm{T}} .* \boldsymbol{z}^{\mathrm{T}}); \tag{32a}$$

$$\boldsymbol{a}_{1\mathrm{mc}(i+1)} = \boldsymbol{a}_{1\mathrm{mc}(i)} + \eta_2 \boldsymbol{C}_{1\mathrm{mc}}[\boldsymbol{W}^{\mathrm{T}} .* \boldsymbol{B}^{\mathrm{T}} .* \boldsymbol{e}_i^{\mathrm{T}} .* (1 - \boldsymbol{z})^{\mathrm{T}}]; \tag{32b}$$

where

$$\boldsymbol{z}_1 = \boldsymbol{a}_{1\mathrm{ma}}^{\mathrm{T}} \boldsymbol{C}_{\mathrm{ma}} - \boldsymbol{a}_{1\mathrm{mc}}^{\mathrm{T}} \boldsymbol{C}_{1\mathrm{mc}}; \tag{33a}$$

$$\boldsymbol{z}_2 = \boldsymbol{a}_{2\mathrm{ma}}^{\mathrm{T}} \boldsymbol{C}_{2\mathrm{ma}} - \boldsymbol{a}_{2\mathrm{mc}}^{\mathrm{T}} \boldsymbol{C}_{2\mathrm{mc}}; \tag{33b}$$

$$\boldsymbol{z}_3 = \boldsymbol{a}_{2\mathrm{a}}^{\mathrm{T}} \boldsymbol{C}_{2\mathrm{a}}; \tag{33c}$$

$$\boldsymbol{z} = \boldsymbol{z}_2 .* \boldsymbol{z}_3 + \boldsymbol{a}_{2\mathrm{mc}}^{\mathrm{T}} \boldsymbol{C}_{2\mathrm{mc}}. \tag{33d}$$

4.2 Design Example

Example 3. For illustration purpose, we applied the optimization approach to design a two-stage FRM filter with the same design parameters as the 3rd example in [13], i.e., $\omega_{\mathrm{p}} = 0.6\pi$, $\omega_{\mathrm{a}} = 0.61\pi$, $N_{2\mathrm{a}} = 27$, $N_{2\mathrm{ma}} = 13$, $N_{2\mathrm{mc}} = 27$, $N_{1\mathrm{ma}} = 15$, $N_{1\mathrm{mc}} = 23$, and $M = 4$. Set $\delta_{\mathrm{p}}/\delta_{\mathrm{s}} = 1$ and $L = 900$. It takes 2800 training iterations (the computation cost 15.4 seconds on a CPU of Pentium4) to converge. The amplitude responses of the various subfilters are shown in Fig.6. The maximum passband ripple is found to be 0.0300dB and the minimum stopband attenuation is 49.04dB. In [13], the passband ripple and stopband attenuation are 0.0320dB and 48.77dB, respectively. Finally, we remark that although the design resulted in a slightly more economical FRM filter compared to the one in Example 1, the two-stage filter offers better performance in both passband and stopband as is evident in Figs. 6(e) and 6(f). Nevertheless, the performance gain is achieved at the cost of an increased group delay $D = 271$ compared to the group delay $D = 218$ for the filter in Example 1.

5 Conclusion

In this paper, a two-step optimization technique has been proposed for the design of the basic and multistage FRM based linear-phase FIR digital filters. An initial FRM filter is generated at first step by alternately optimizing the subfilters with the aid of a simple standard algorithm. At the second step, this solution is then used as a start-up solution for further optimization, in which

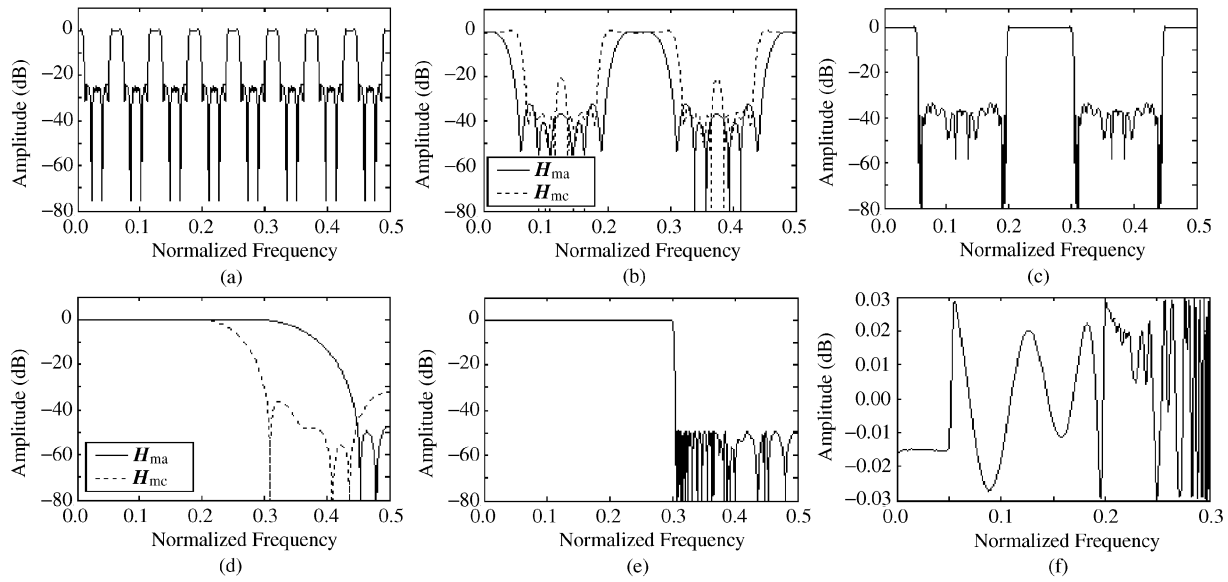

Fig.6. Amplitude responses. (a) Prototype filter $H_{\mathrm{a}}^{(2)}(z^{16})$. (b) Masking filters $H_{\mathrm{ma}}^{(2)}(z^4)$ and $H_{\mathrm{mc}}^{(2)}(z^4)$. (c) "Prototype" filter $H_{\mathrm{a}}^{(1)}(z^4)$. (d) Masking filters $H_{\mathrm{ma}}^{(1)}(z)$ and $H_{\mathrm{mc}}^{(1)}(z)$. (e) FRM filter. (f) Passband ripples of the FRM filter.

the high degree nonlinear optimal problem is decomposed into several linear neural network optimal problems. For each linear optimal problem, a new varying learning rate BBPNN approach is taken. Some examples taken from the literatures have shown that the proposed algorithm can design better FRM filters than several existing methods.

References

[1] Yu Y J, Teo K L, Lim Y C, Zhao G H. Extrapolated impulse response filter and its application in the synthesis of digital filters using the frequency-response masking technique. *Signal Processing*, 2005, 50(3): 581–590.

[2] Furtado M B, Diniz P S R, Netto S L. Optimized prototype filter based on the FRM approach for consine-modulated filter bank. *Circuits, Systems, Signal Processing*, 2003, 22(2): 193–210.

[3] Lim Y C, Yang R. On the synthesis of very sharp decimators and interpolators using the frequency-response masking technique. *IEEE Trans. Signal Processing*, 2005, 53(4): 1387–1397.

[4] Lim Y C. Frequency-response-masking approach for the synthesis of sharp linear phase digital filters. *IEEE Trans. Circuits Syst.*, 1986, 33(4): 357–364.

[5] Lim Y C, Lian Y. The optimum design of one- and two-dimensional FIR filters using the frequency response masking technique. *IEEE Trans. Circuits Syst. II*, 1993, 40(2): 88–95.

[6] Saramäki T, Lim Y C. Use of Remez algorithm for designing FIR filters utilizing the frequency-response masking approach. In *Proc. IEEE Int. Conf. Circuits Syst.*, Orlando, FL, USA, May 30∼Jun. 2, 1999, pp.III449–III455.

[7] Lian Y, Zhang L, Ko C C. An improve frequency response masking approach for designing sharp FIR filters. *Signal Processing*, 2001, 81(12): 2573–2581.

[8] Lim Y C, Lian Y. Frequency-response masking approach for digital filter design: Complexity reduction via masking filters factorization. *IEEE Trans. Circuits Syst. II*, 1994, 41(8): 518–525.

[9] Cen L. Frequency response masking filter design using an oscillation search genetic algorithm. *Signal Processing*, 2007, 87(12): 3086–3095.

[10] Cen L, Lian Y. Hybird genetic algorithm for the design of modified frequency-response masking filters in discrete space. *Circuits, Systems, Signal Processing*, 2006, 25(2): 153–174.

[11] Lu W S, Hinamoto T. Optimal design of FIR frequency-response-masking filters using second-order cone programming. In *Proc. IEEE Int. Symp. Circuits Syst.*, Bangkok, Thailand, May 25∼28, 2003, pp. III878–III881.

[12] Saramäki T, Kaakinen J Y. Optimization of frequency-response masking based FIR filters. *Journal of Circuits, Systems, and Computers*, 2003, 12(5): 563–591.

[13] Lu W S, Hinamoto T. Optimal design of frequency-response masking filters using semidefinite programming. *IEEE Trans. Circuits Syst. II*, 2003, 50(4): 557–568.

[14] Lee W R, Rehbock V, Teo K L. A weight least-square-based approach to FIR filter design using the frequency-response masking technique. *IEEE Signal Processing Letters*, 2004, 11(7): 593–596.

[15] Lee W R, Rehbock V, Teo K L, Caccetta L. A weight least-square-based approach to FIR filters synthesized using the modified frequency response masking structure. *IEEE Trans. Circuits Syst. II*, 2006, 53(5): 379–383.

[16] Lee W R, Caccetta L, Teo K L, Rehbock V. A Unified Approach to Multistage Frequency- Response Masking Filter Design using the WLS Technique. *IEEE Trans. Signal Processing*, 2006, 54(9): 3459–3467.

Xiao-Hua Wang was born in 1968. He is an associate professor of Electrical and Information Engineering College, Changsha University of Science & Technology, since 2004. At present he is a Ph.D. candidate of Hunan University, and he has published more than 30 papers on his researches. His research interests include neural networks theory and application, digital filters design, computer monitoring and signal processing.

Yi-Gang He was born in 1966. He received his Ph.D. degree in electrical engineering from Xi'an Jiaotong University in 1996. He has been a full professor of electrical engineering at Hunan University, China, Since 1999. He was a senior visiting scholar at the University of Hertfordshire, UK, in 2002. Currently, he is the director of the Institute of Testing Technology for Circuits & Systems at Hunan University. He has published over 100 papers on his researches. His teaching and research interests are in the areas of circuit theory and its applications, testing and fault diagnosis of analog and mixed-signal circuits, and signal processing.

Tian-Zan Li received her B.S. degree in electronic information and technology from Hunan University in 2004. She is currently a graduate student of Changsha University of Science and Technology. Her fields of interests include power system measurement, power system harmonious analysis.